ISSN: 0974-5823 Vol. 7 No. 4 April, 2022

International Journal of Mechanical Engineering

Modeling the Behavior of Undrained Banding Sand by the Implementation of Generalized Plasticity in the Micro-Planes Framework

Meysam Zarinfar

Department of Civil Engineering, Bu-Ali Sina University, Hamedan, Iran

ABSTRACT

The Pastor-Zienkiewicz constitutive model capable of predicting sand behavior under static and dynamic loading has been implemented in the micro-plane framework in this article. The proposed model can simulate stress-strain history on micro-planes in materials. Model verification under different loading/unloading/reloading stress-strain paths (undrained triaxial test) has been examined, and the failure direction of sand samples has been specified. Hence, the proposed constitutive model can be used to predict strain localization.

Keywords: constitutive relation, generalized plasticity, micro-plane, undrained triaxial test

INTRODUCTION

The micro-plane is a plane in material with different orientations. The micro-plane predicts the constitutive behavior on a micro-scale. Taylor [1] proposed slip planes as the first idea for this model. Batdorf and Budiansky [2] formulated Taylor's model in detail. The micro-plane framework has been used for other materials such as metals, soils, and rocks. The static constraint was the base of the micro-plane or multi-laminate models before 1984. In this approach, the proof of compatibility condition is not a simple task. Bazant and coworkers [3] projected strain instead of the stress on micro-planes. Therefore, compatibility condition is satisfied by introducing the kinematic constraint approach. Finally, the equilibrium condition is established by using the principle of virtual work. This constitutive model has been used recently in scientific research [6, 7].

The Pastor-Zienkiewicz constitutive model has been implemented in the micro-plane framework in this article. The proposed model is a combination of generalized plasticity and the micro-plane framework. The model is verified under different undrained triaxial tests. The failure direction of sand samples has been specified, and the ability of the proposed constitutive model has been examined in the prediction of strain localization.

Micro-plane formulation

The virtual work done on volume V by stress can be obtained from the following integral relation.

$$\delta \dot{W} = \int_V \dot{\sigma}_{ij} \delta\varepsilon_{ij} \quad . \tag{1}$$

Furthermore, the strain is resolved into tangential and normal directions.

$$d\varepsilon_n = d\varepsilon_N + d\varepsilon_T, \quad (d\varepsilon_n)_i = n_k d\varepsilon_{ik}, \quad (d\varepsilon_N)_i = n_i n_j n_k d\varepsilon_{jk}, \quad (d\varepsilon_T)_i = (n_k \delta_{ij} - n_i n_j n_k) d\varepsilon_{jk} . \tag{2}$$

The principle of virtual work requires that:

$$\delta \dot{W} = \frac{4\pi}{3} \dot{\sigma}_{ij} \delta\varepsilon_{ij} = 2\int_A (\dot{\sigma}_N \delta\varepsilon_N + \dot{\sigma}_T \delta\varepsilon_T) dA \quad . \tag{3}$$

where A is the surface of the volume V. The following equations are written based on the constitutive relation.

$$\dot{\sigma}_N = D^{ep}_{NN} \dot{\varepsilon}_N + D^{ep}_{NT} \dot{\varepsilon}_T, \quad \dot{\sigma}_T = D^{ep}_{TN} \dot{\varepsilon}_N + D^{ep}_{TT} \dot{\varepsilon}_T \quad . \tag{4}$$

Then, the equation (3) takes the form:

$$\dot{\sigma}_{ij} \delta\varepsilon_{ij} = \frac{3}{2\pi} \int_A \left[(D^{ep}_{NN} \dot{\varepsilon}_N + D^{ep}_{NT} \dot{\varepsilon}_T) \delta\varepsilon_N + (D^{ep}_{TN} \dot{\varepsilon}_N + D^{ep}_{TT} \dot{\varepsilon}_T) \delta\varepsilon_T \right] dA \quad . \tag{5}$$

The derivative of strain on each plane with respect to macroscopic strain tensor can be calculated as:

$$\frac{\partial \varepsilon_N}{\partial \varepsilon_{ij}} = n_i n_j = A_{ij}\ , \quad \frac{\partial \varepsilon_T}{\partial \varepsilon_{ij}} = \frac{n_j n_r}{\varepsilon_T}\left(\varepsilon_{ir} - n_i n_s \varepsilon_{rs}\right) = B_{ij} \quad . \tag{6}$$

By substituting equation (6) into equation (5), the stress-strain rate relation can be obtained:

$$\dot{\sigma}_{ij} = \frac{3}{2\pi}\int_A \left[\left(D^{ep}_{NN}A_{rs} + D^{ep}_{NT}B_{rs}\right)A_{ij} + \left(D^{ep}_{TN}A_{rs} + D^{ep}_{TT}B_{rs}\right)B_{ij}\right]\dot{\varepsilon}_{rs}\,dA \quad . \tag{7}$$

The integration in equation (7) on the surface of the volume is calculated by the Gaussian technique. This integration method considers a limited number of micro-planes. In other words, there is one micro-plane for each integration point. 34 Gaussian points are used in this study for numerical analysis.

The cosine angle and weight factor of integration points are shown in Table 1.

$$\dot{\sigma}_{ij} = 6\sum_{\beta=1}^{n} w_\beta \left[\left(D^{ep}_{NN}A_{rs} + D^{ep}_{NT}B_{rs}\right)A_{ij} + \left(D^{ep}_{TN}A_{rs} + D^{ep}_{TT}B_{rs}\right)B_{ij}\right]_\beta \left(\dot{\varepsilon}_{rs}\right)_\beta = 6\sum_{\beta=1}^{n} w_\beta \left(D^{ep}_{ijrs}\right)_\beta \left(\dot{\varepsilon}_{rs}\right)_\beta \quad . \tag{10}$$

Table 1: Cosine angle and weight factor of micro-planes ($a=1$, $b=\sqrt{2}/\sqrt{3}$, $c=\sqrt{2}/2$, $d=\sqrt{3}/3$, $e=\sqrt{6}/6$, $f=0$, $w_1=.058130468$, $w_2=.038296881$, $w_3=.030091134$, $w_4=.029390060$, $w_5=.020277985$, $w_6=.019070616$)

Plane No		1	2	3	4	5	6	7	8	9	10	11	12	13	14	15	16	17
normal axis	n_1	d	d	-d	-d	c	-c	c	-c	f	f	a	f	f	e	e	-e	-e
	n_2	d	-d	d	-d	c	c	f	f	-c	c	f	a	f	e	-e	e	-e
	n_3	d	d	d	d	f	f	c	c	c	c	f	f	a	b	b	b	b
w_i		w_5	w_5	w_5	w_5	w_1	w_1	w_3	w_3	w_3	w_3	w_2	w_2	w_4	w_6	w_6	w_6	w_6

Pastor-Zienkiewicz constitutive model

Zienkiewicz and Morz [4] introduced the generalized plasticity theory. Pastor and Zienkiewicz [4] extended the framework to simulate the behavior of sand under different stress paths, including monotonic and cyclic conditions. In this theory, the stress-strain relation in loading differs from the unloading conditions. By the combination of micro-plane and generalized plasticity theory, the increments of stress on micro-planes under loading/unloading paths are written as follows:

$$\begin{bmatrix} d\sigma_N \\ d\sigma_T \end{bmatrix}_{L/U} = \begin{bmatrix} D^{ep}_{NN} & D^{ep}_{NT} \\ D^{ep}_{TN} & D^{ep}_{TT} \end{bmatrix}_{L/U} \begin{bmatrix} d\varepsilon_N \\ d\varepsilon_T \end{bmatrix}_{L/U} = D^{ep}_{L/U} \begin{bmatrix} d\varepsilon_N \\ d\varepsilon_T \end{bmatrix}_{L/U}, \quad D^{ep}_L = D_e - \frac{D_e.n_{gL}.n^T.D_e}{H_L + n^T.D_e.n_{gL}} \quad . \tag{12}$$

Plastic strain in generalized plasticity is calculated by the equation (13):

$$d\varepsilon^p = \left(\frac{n^T D^e d\varepsilon}{H + n^T D^e n_g}\right) n_g \tag{13}$$

$$H = H_0 P' H_f(H_v) H_{dm} \tag{14}$$

$$H_0 = \frac{1+e_0}{\lambda(0)-k} \tag{15}$$

$$H_f = (1-\frac{\eta}{\eta_f}) \qquad \eta_f = (1+\frac{1}{c})M_f \tag{16}$$

$$H_v = (1-\frac{\eta}{M_g}) \tag{17}$$

$$H_s = \beta_0\beta_1 \exp(-\beta_0\xi) \tag{18}$$

$$H_{dm}=\left(\frac{\zeta_{\max}}{\zeta}\right)^{\gamma} \qquad \zeta=p'\left[1-(\frac{1}{1+c})\frac{\eta}{M}\right]^{\frac{1}{c}} \tag{19}$$

For more information about constitutive model parameters, see reference [4]

Numerical simulation

In this section, the behavior of Banding sand is examined by the proposed model. For this purpose, the undrained behavior of Banding sand with different relative densities is considered. The values of the model parameters are shown in Table 2. Elastic properties are considered the same as reference 4, because only the plastic strain is projected on micro-planes. As shown in Fig 1 and Fig 4, Numerical analysis simulates experimental values with sufficient accuracy.

Table 2: Model Parameters used in simulations

Dr	k_{ev0}(KPa)	G_0(KPa)	M_f	M_g	H_0	β_0	β_1	γ	H_{u0}	γ_u
29%	35000	525000	.27	1.5	2450	4.2	.2	2.5	3500000	1
44%	35000	525000	.27	.6	7000	4.2	.2	-	-	-
47%	35000	525000	.27	.48	12250	4.2	.2	-	-	-
66%	35000	525000	.27	.44	26250	4.2	.2	-	-	-

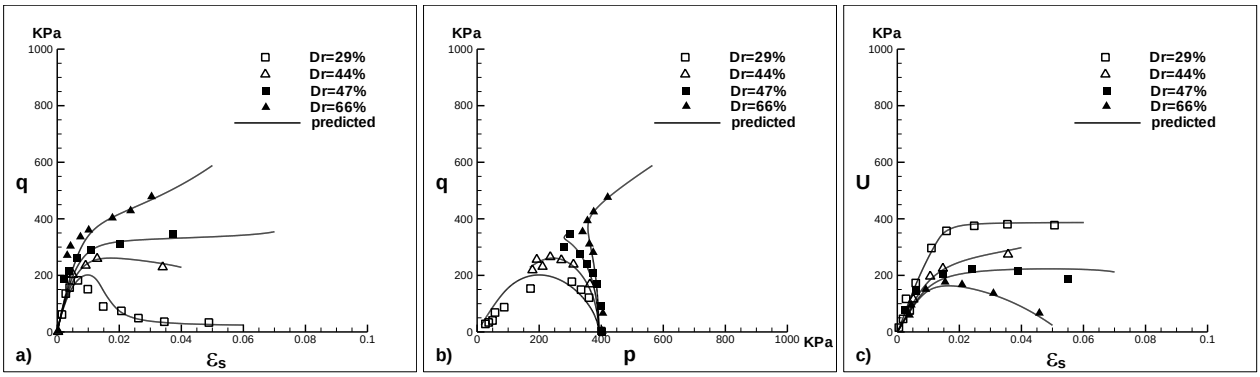

Figure (1) behavior of Banding sand in Undrained condition a) deviatoric stress b) stress path, c) pore pressure.

The maximum value of tangential strain in the sample with a relative density of .29 occurs on planes numbers 14, 15, 16, and 17 (Fig 2(b)). In other words, strain localization is created on these planes. The collapse of soil occurred when the stress state reached the Mohr-Coulomb line. In this case, the stress path on the micro-planes numbers 14, 15, 16, and 17 intersects with the failure line (Fig 2(c)). The tangential strain value on the other micro-planes is fewer amounts than on planes with the numbers 14, 15, 16, and 17. This indicates that the strain localization or shear band of loose sand occurs on micro-planes numbers 14 to 17. The highest value of the normal plastic strain occurs on planes number 14, 15, 16, and 17 (Fig 2(a)). This happened because the loose sand contracts under shear loading.

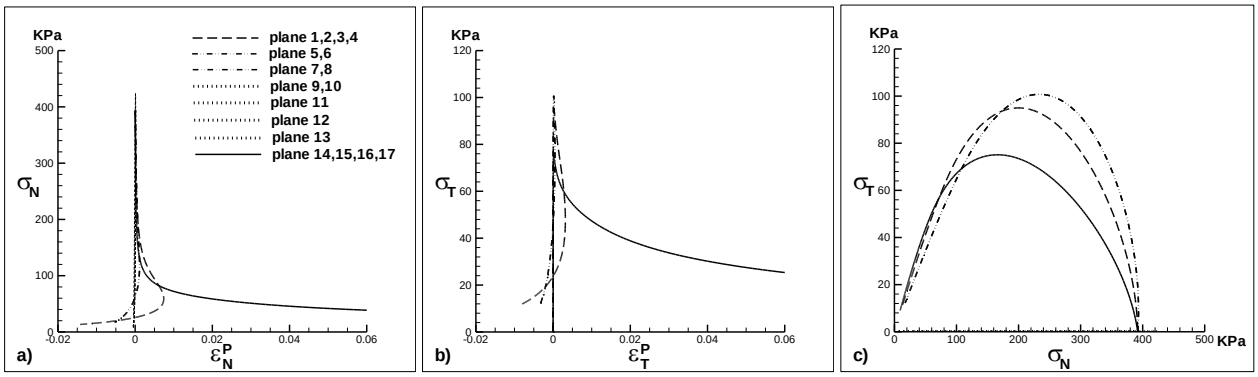

Figure (2) a) normal stress b) tangential stress c) stress path (Dr=.29)

With the increased in relative density, the tangential strain on several micro-planes becomes significant. These sets of micro-planes are represented by (1 to 4), (5 to 8), and (14 to17). As shown in Fig 3(c), stress paths on micro-plane numbers (1 to 4) and (14 to 17) are critical.

This means that the failure orientation may be located between these sets of micro-planes and is closer to micro-planes numbers 1, 2, 3, 4. The tangential strain on these micro-planes has the highest amount. As seen in experimental results [5], the orientation of the

failure plane increases with the increased in relative density. The agreement of the obtained results with the laboratory results shows the accuracy and efficiency of the numerical model. With the increasing of relative density, the normal plastic strain on micro-planes decreases because the dense sand dilates under shear loading.

Simulation of Banding sand under the cyclic loading is shown in Fig 4. Because Pastor–Zienkiewicz model has the ability to model important features of sand, model prediction is in good agreement with experimental results. As mentioned before, the strain localization of loose sand occurs on micro-planes numbers 14 to 17 (Fig 5).

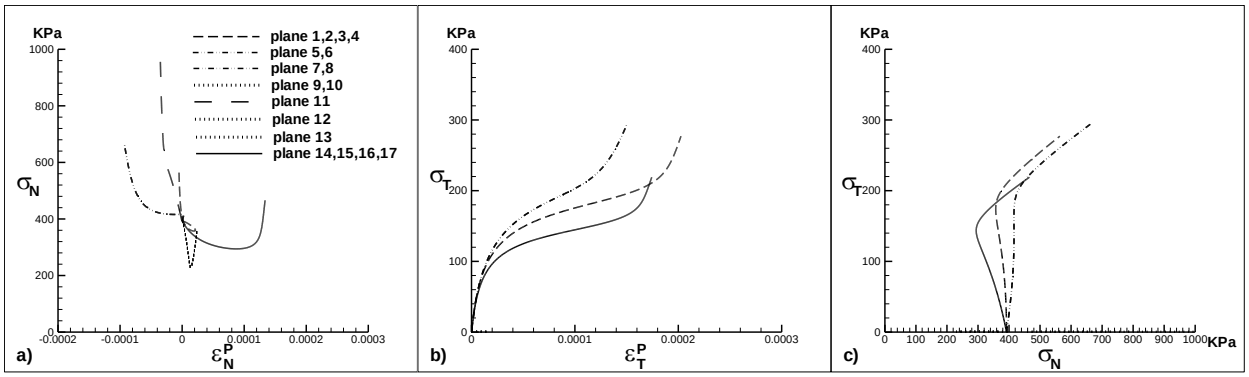

Figure (3) a) normal stress b) tangential stress c) stress path (Dr=.66)

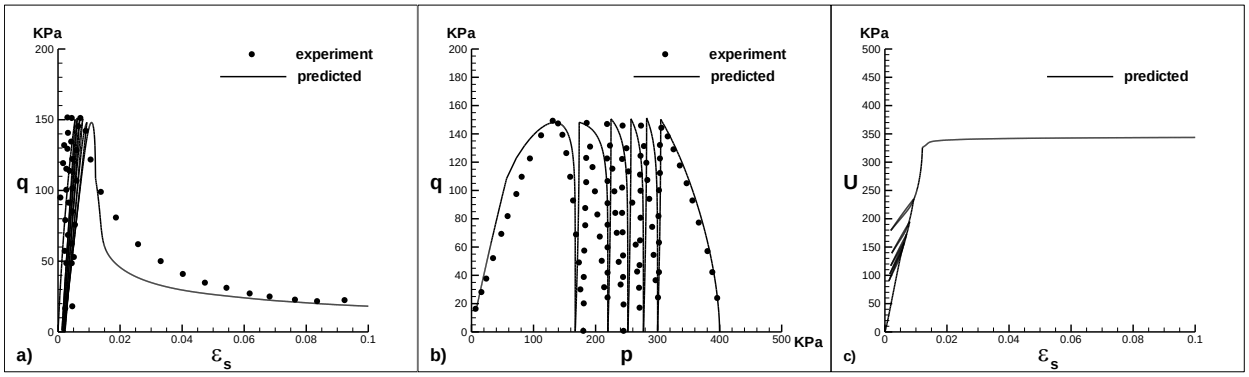

Figure (4) behavior of Banding sand in Undrained condition (Dr=.29) a) deviatoric stress b)stress path, c) pore pressure.

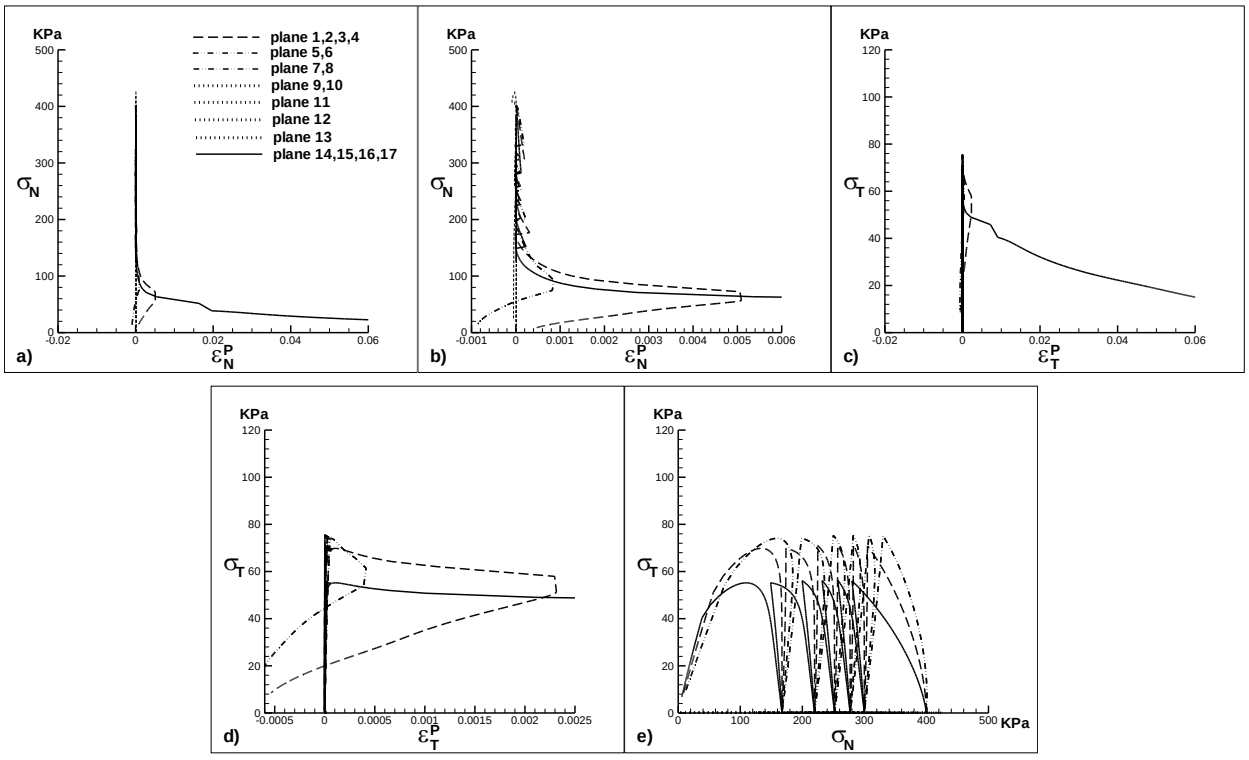

Figure (5) a,b) normal stress c,d) tangential stress e) stress path (Dr=.29)

CONCLUSION

A constitutive model has been proposed using the combination of the micro-plane and generalized plasticity theory. The Pastor-Zienkiewicz constitutive model capable of predicting sand behavior has been used. The suggested constitutive model projects stress-strain history on micro-planes in materials. The agreement of the obtained results with the laboratory results shows the accuracy and efficiency of the numerical model. Failure direction of loose and dense sand samples is specified. Simulation results indicate that the orientation of the shear band increases with the increased in relative density.

References

[1] Bragg, W. L. (1938). A discussion on plastic flow in metals. *Proceedings of the Royal Society of London. Series A. Mathematical and Physical Sciences*, *168*(934), 302-317.

[2] Batdorf, S. B., & Budiansky, B. (1949). *A mathematical theory of plasticity based on the concept of slip* (No. NACA-TN-1871).

[3] Bažant, Z. P., & Gambarova, P. G. (1984). Crack shear in concrete: Crack band microflane model. *Journal of structural engineering*, *110*(9), 2015-2035.

[4] Pastor, M., Zienkiewicz, O. C., & Chan, A. (1990). Generalized plasticity and the modelling of soil behaviour. *International Journal for numerical and analytical methods in geomechanics*, *14*(3), 151-190.

[5] Alshibli, K. A., & Sture, S. (2000). Shear band formation in plane strain experiments of sand. *Journal of geotechnical and geoenvironmental engineering*, *126*(6), 495-503.

[6] Vorel, J., Marcon, M., Cusatis, G., Caner, F., Di Luzio, G. and Wan-Wendner, R., 2021. A comparison of the state of the art models for constitutive modelling of concrete. *Computers & Structures*, *244*, p.106426..

[7] Xue, J. and Kirane, K., 2022. Cylindrical microplane model for compressive kink band failures and combined friction/inelasticity in fiber composites I: Formulation. *Composite Structures*, *289*, p.115382.